Supporting Information for:

Pyrazolyl methyls prescribe the electronic properties of iron(II) tetra(pyrazolyl)lutidine chloride complexes.

Tyler J. Morin, Sarath Wanniarachchi, Chengeto Gwengo, Vitales Makura, Heidi M. Tatlock, Sergey V. Lindeman, Brian Bennett, Gary J. Long, Fernande Grandjean, and James R. Gardinier*.

Table of Contents:

Figure S1. Top**:** Pictures of a crystal of **1**·CH_2Cl_2 highlighting representative thermochromic behavior and comparison of 270 (red wireframe) and 100 K (blue wireframe) structures. Bottom: 270 K structure with atom labeling used for metrics in Table1 of main text.

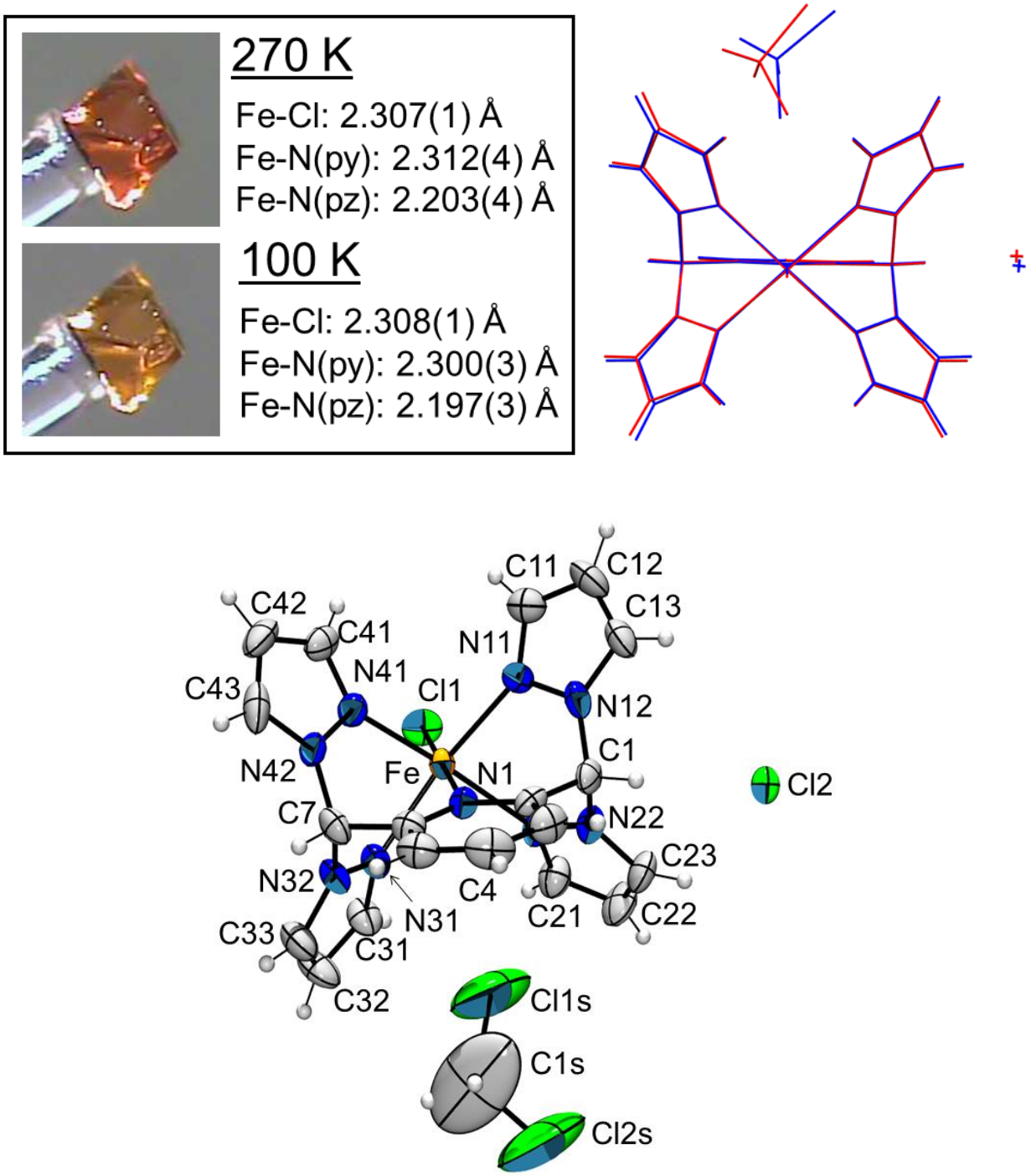

Figure S2. Structure of **1**·MeOH and partial atom labeling used for metrics in Table1 of main text.

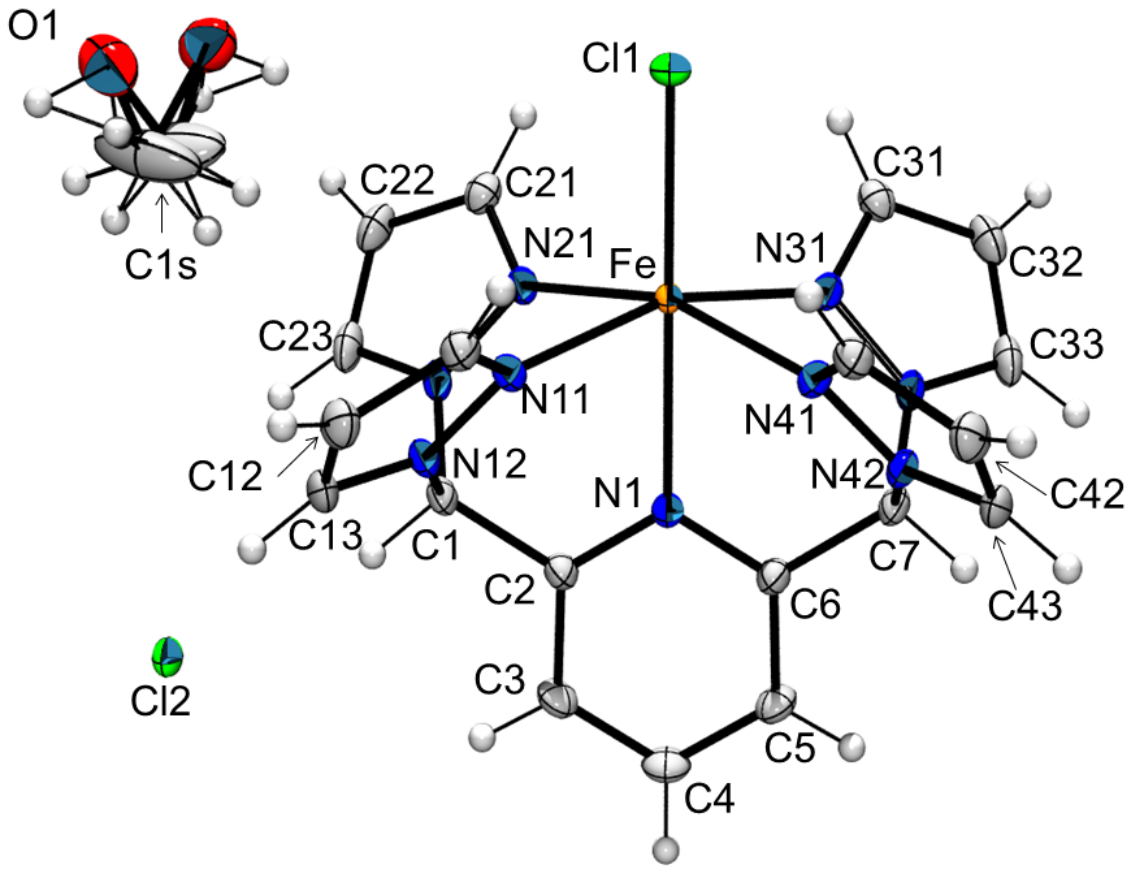

Figure S3. Structure **1**·2MeOH and partial atom labeling used for the metrics in Table 1 of main text.

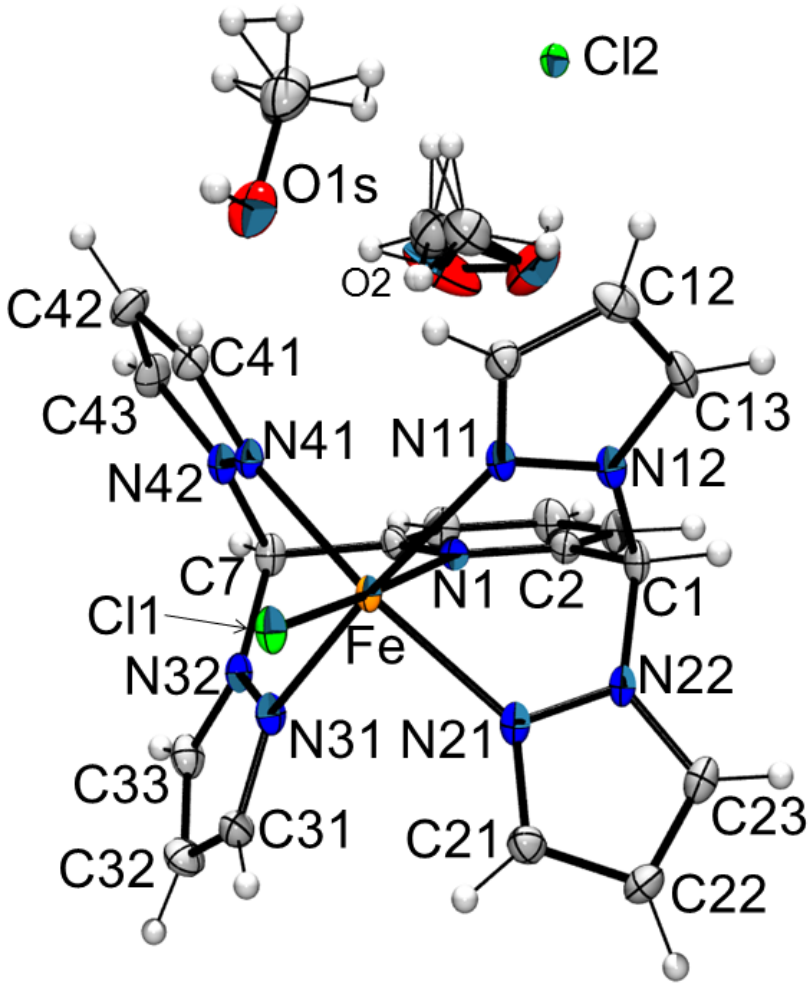

Figure S4. Structure of **2**·MeOH·0.35Et_2O and partial atom labeling used for the metrics in Table 1 of main text.

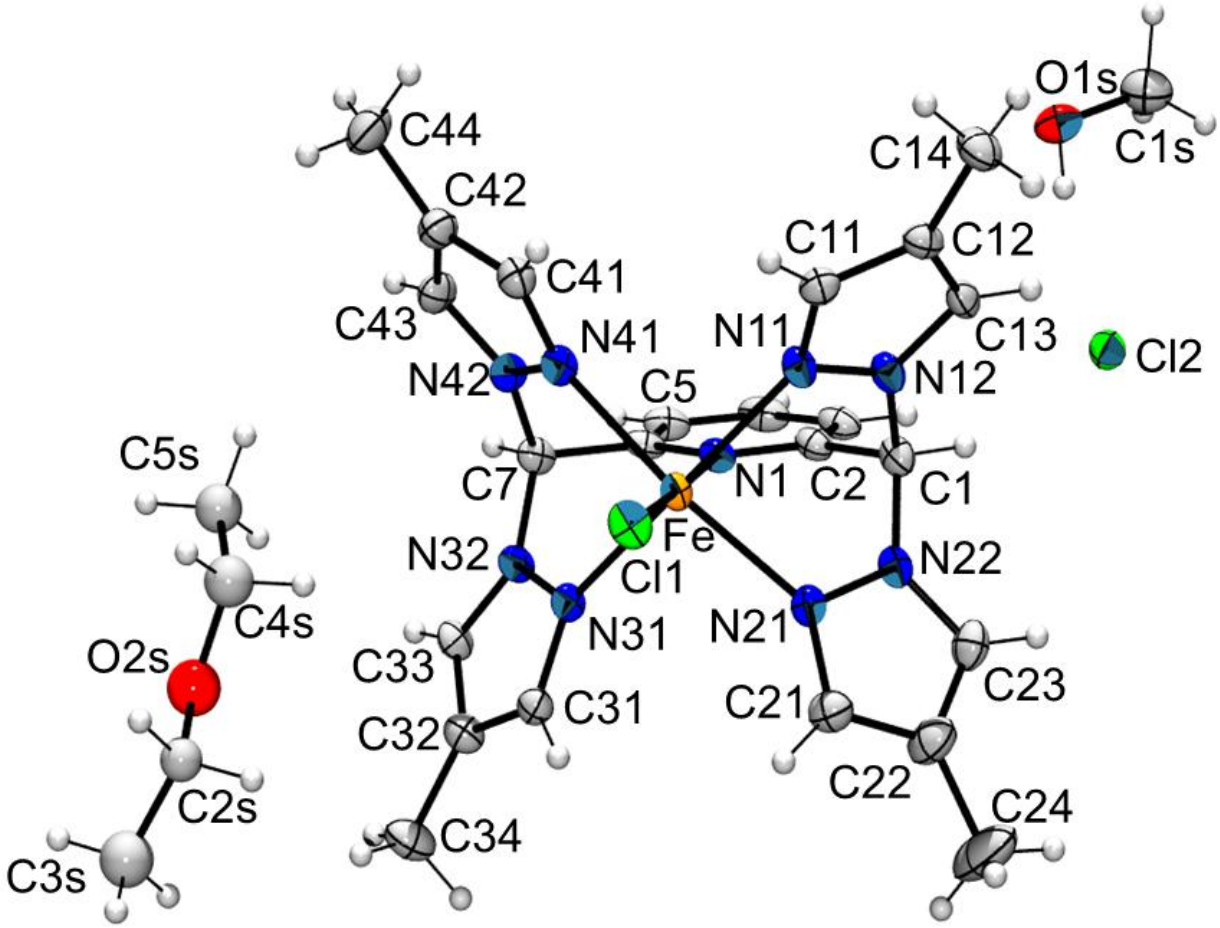

Figure S5. Structure of **3**·MeOH and partial atom labeling used for the metrics in Table 1 of main text.

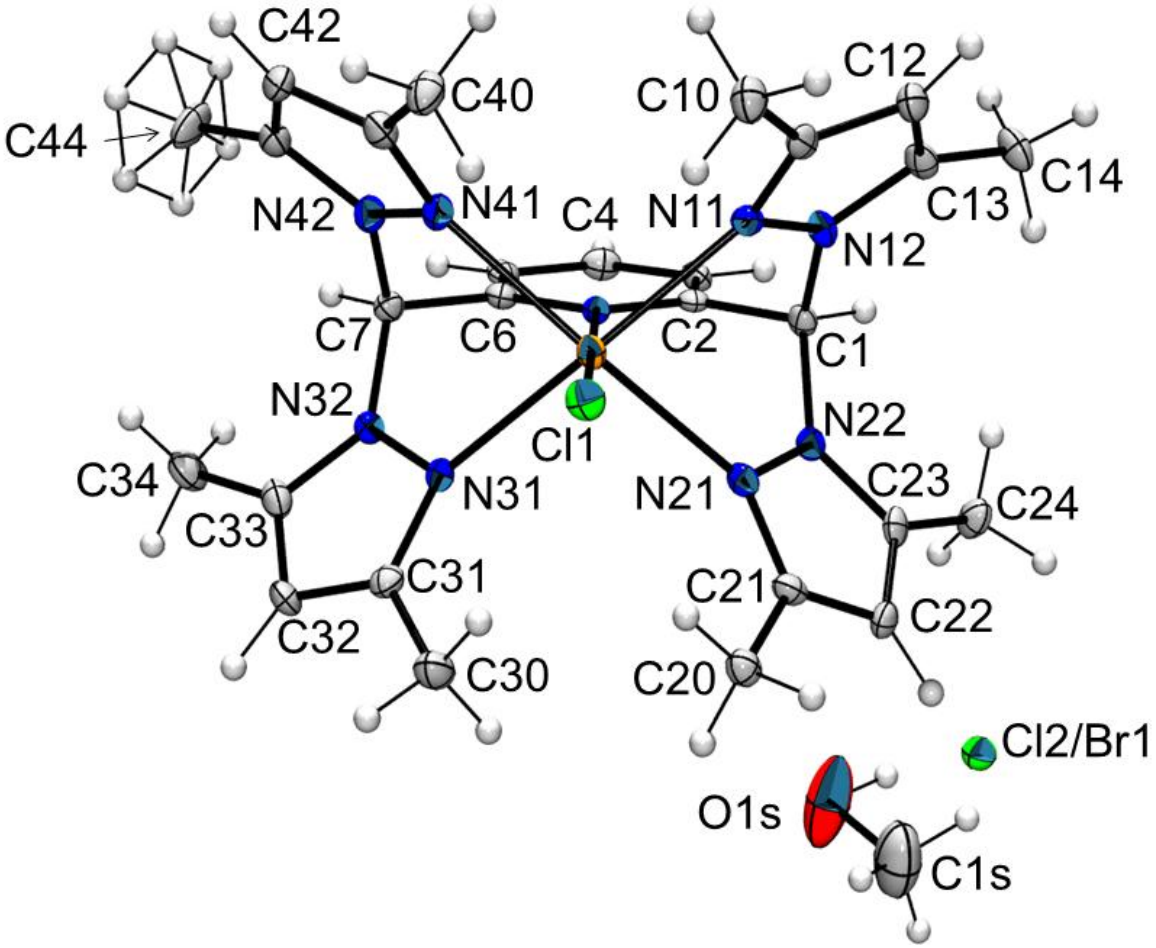

Figure S6. Structure of **3**·2MeOH and atom labeling used for the metrics in Table 1 of main text.

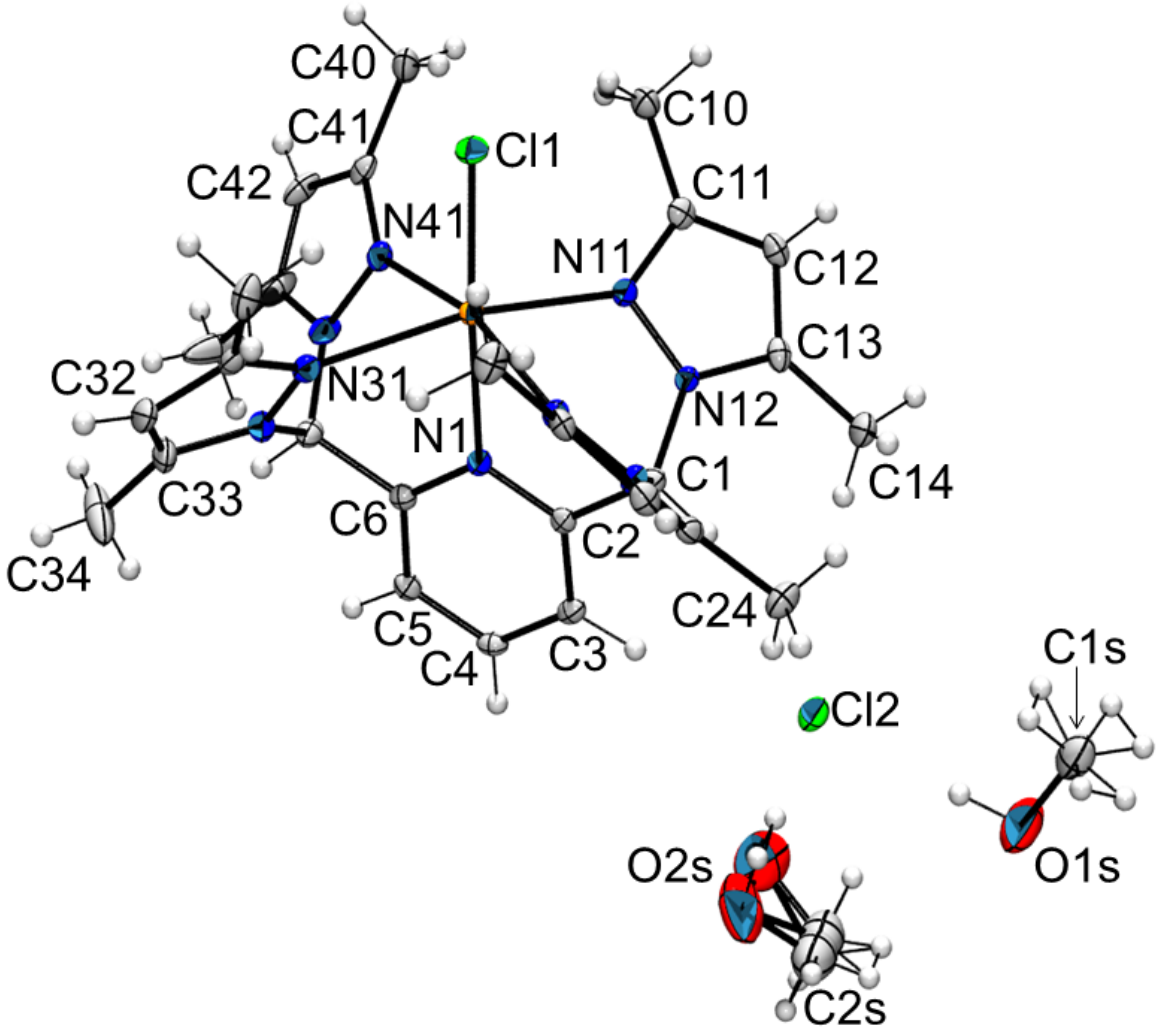

Figure S7. (A) Structure of cation with hydrogens removed for clarity and (B) view of asymmetric unit in **4**·1.75MeOH.

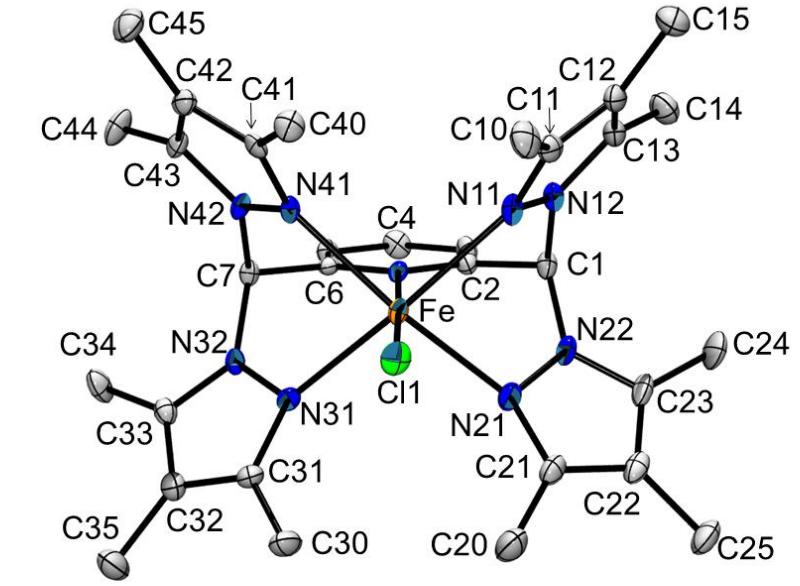

(A)

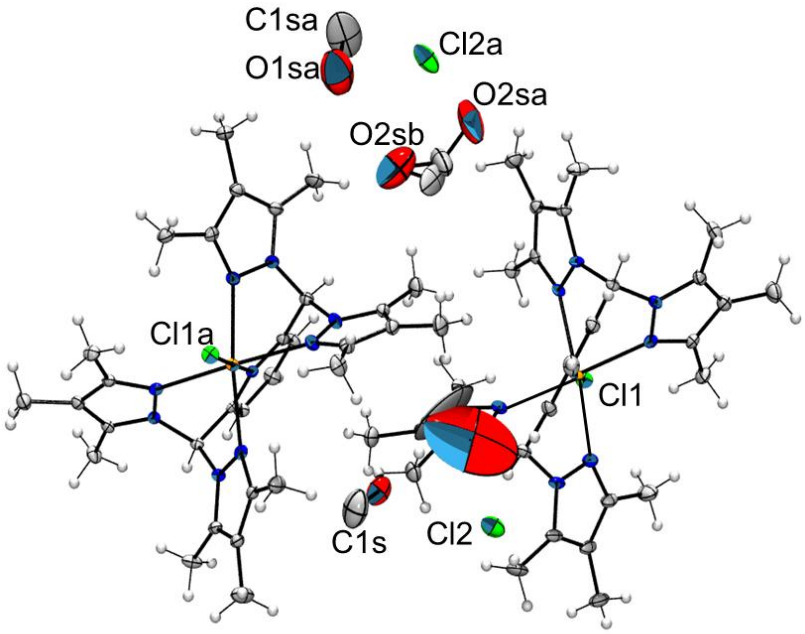

(B)

[B] Powder X-Ray Diffraction.

Figure S8. Calculated powder X-ray diffraction pattern for **2**·MeOH·0.35Et_2O (blue line, bottom) and observed pattern (black line, top) from as-isolated, ground powder before exposure to Et_2O.

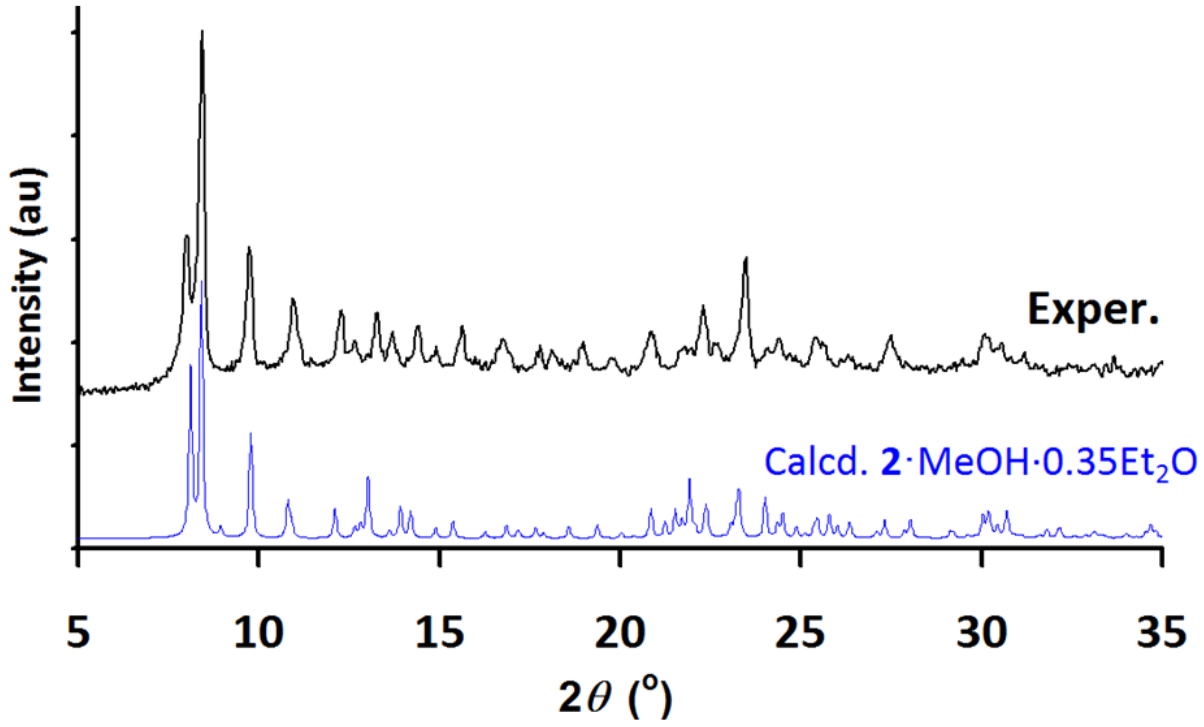

Figure S9. Calculated powder X-ray diffraction pattern for **3** (blue, middle and dashed violet, bottom, lines) and observed pattern for ground powder (black, top)**.**

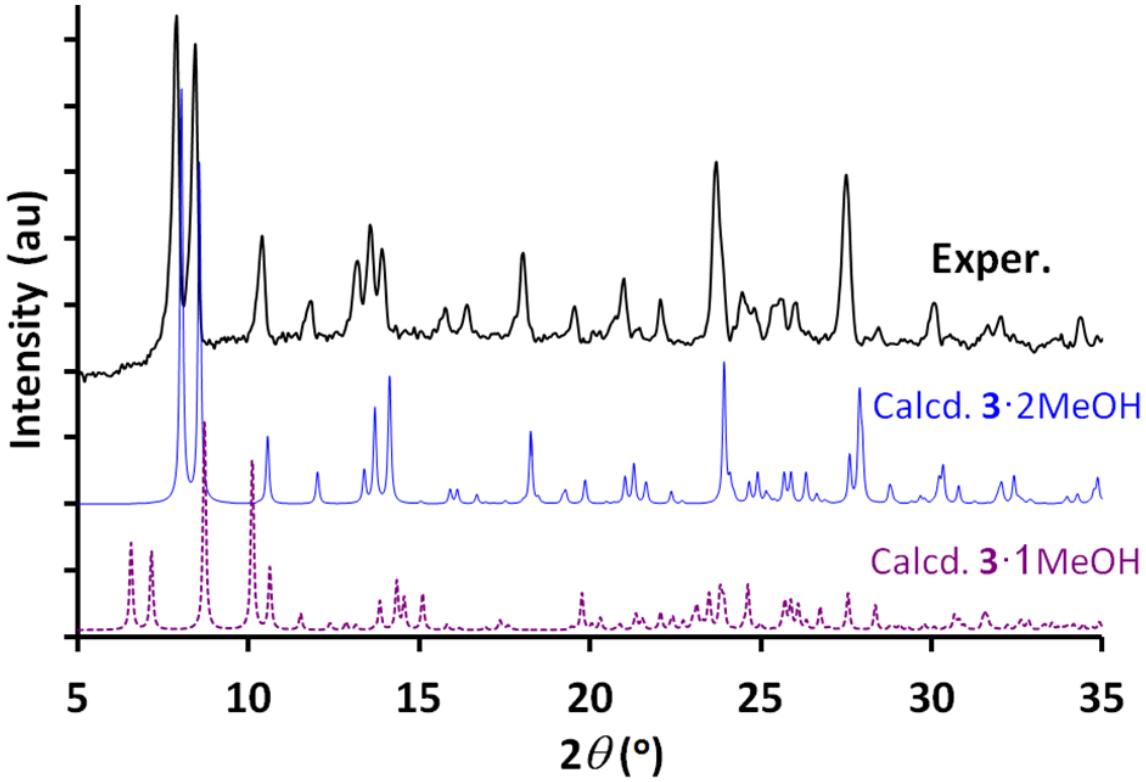

Figure S10. Calculated powder X-ray diffraction pattern for **4**·1.75MeOH (blue line, bottom) and observed data from as-isolated, ground powder(black, top)**.**

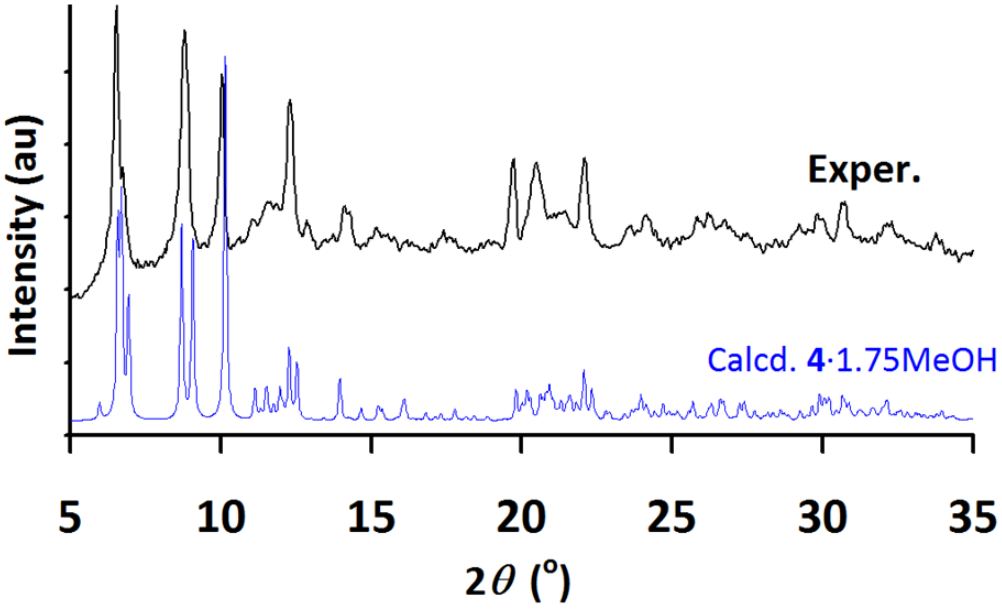

[C] Electronic Spectra.

Figure S11. Vis-NIR electronic spectra for **1-3** with representative isomolar titration (Job's) plots for **1**-**4**.

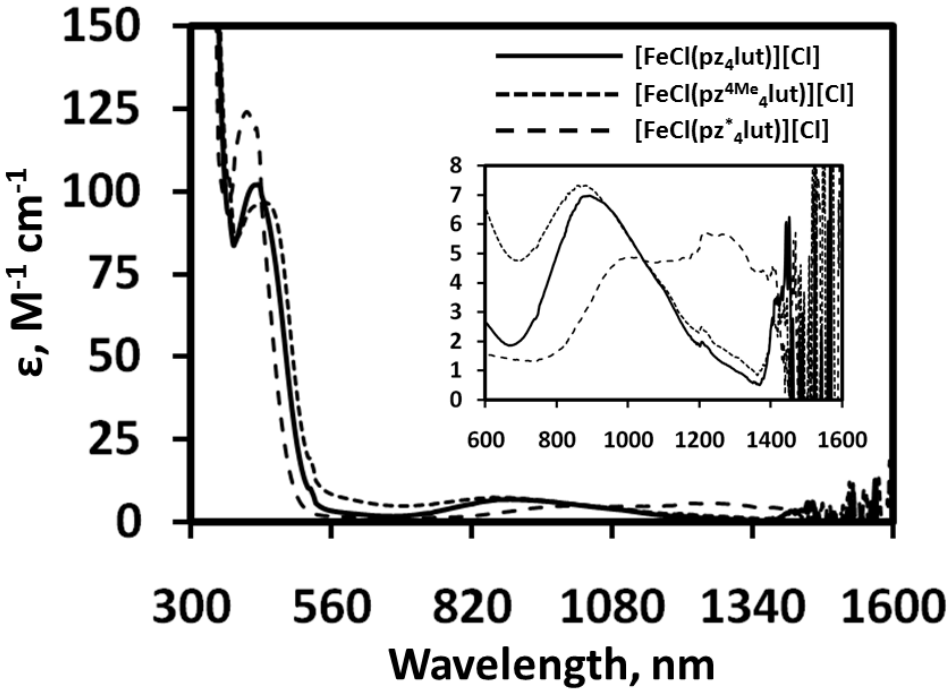

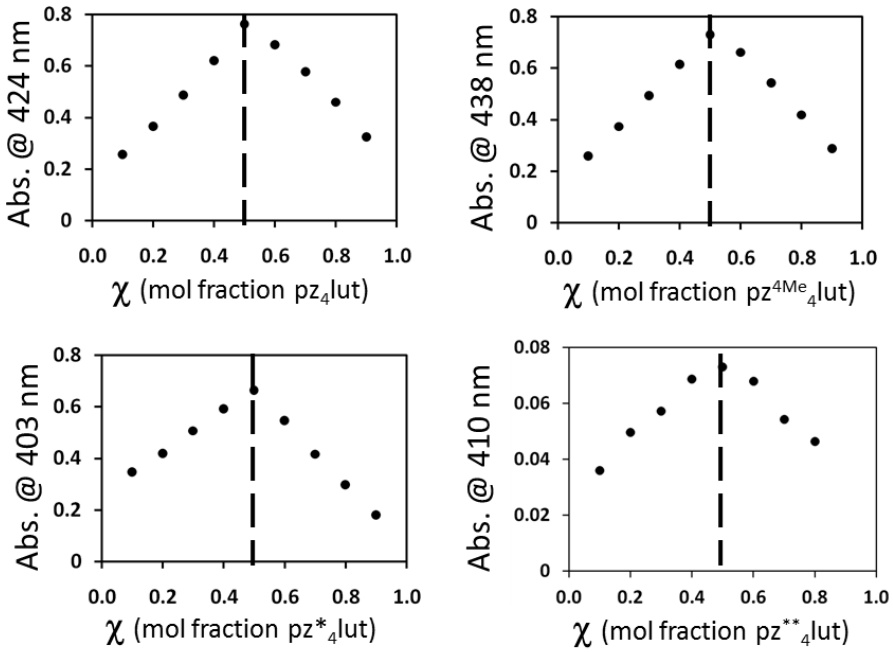

[D] EPR Spectroscopy.

EPR measurements were obtained using a Bruker ELEXSYS E600 equipped with an ER4116DM cavity resonating at 9.63 GHz, an Oxford Instruments ITC503 temperature controller and ESR-900 helium-flow cryostat. The EPR spectra were recorded with 100 kHz field modulation. It was previously discovered that **1**·CH_2Cl_2 was a rare example of a non-Kramer's (S = 2) system that gave a detectable EPR signal owing to some proportion of the zero-field splitting envelope satisfying the condition $\Delta < 0.3$ cm^{-1}.[S1] Therefore, the X-band (9.6 GHz) electron paramagnetic resonance spectra for the high-spin complexes **2-4** were obtained at 10 K in 9:1 MeOH:EtOH in both perpendicular and parallel modes. The EPR spectra for each complex (Figure S12) gave a broad signal with g>>2 consistent with high-spin iron(II); hyperfine structure was not observed. The sharp signal near g = 4 observed in the perpendicular mode spectrum of each complex broadens in the parallel mode, indicative of a minor Fe(III) impurity in the samples. The g-values decreases with decreasing ligand field strength with g ~9.5 for **2**·MeOH·0.35Et_2O, ~8.0 for **1**·CH_2Cl_2 and ~4.0 for **3**·2MeOH.

Figure S12. Perpendicular mode (left) and parallel mode (right) X-band EPR of **1**•CH_2Cl_2, bottom, **2**·MeOH·0.35Et_2O, middle, and **3**·2MeOH, top, at 3 mW and 10 K.

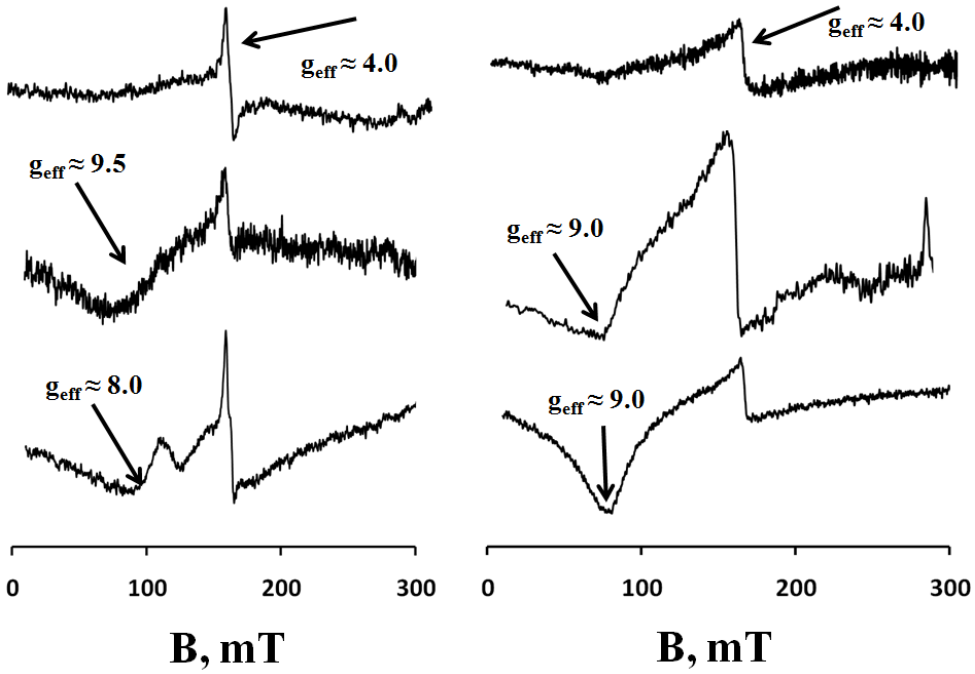

[E] References.

[S1] T. J. Morin, B. Bennett, S.V. Lindeman, J. R. Gardinier, *Inorg. Chem.* 2008, ***47***, 7468.